NASA MEMO 2-4-59A

NASA

MEMORANDUM

NORMAL-FORCE AND PITCHING-MOMENT CHARACTERISTICS FOR TWO BLUNT-NOSED RE-ENTRY TYPE BODIES FROM M = 2.4 TO M = 4.0

By Charles E. DeRose

Ames Research Center
Moffett Field, Calif.

NATIONAL AERONAUTICS AND SPACE ADMINISTRATION

WASHINGTON

February 1959

NATIONAL AERONAUTICS AND SPACE ADMINISTRATION

MEMORANDUM 2-4-59A

NORMAL-FORCE AND PITCHING-MOMENT CHARACTERISTICS FOR TWO BLUNT-NOSED RE-ENTRY TYPE BODIES FROM M = 2.4 TO M = 4.0*

By Charles E. DeRose

SUMMARY

Tests were made to investigate the linearity of the pitching-moment and normal-force curves of two blunt-nosed bodies. Test Mach numbers were 2.4 to 4.0 and Reynolds numbers, based on base diameter, were 0.7 to 2.0×10^6. The variation of normal force and pitching moment with angle of attack was obtained for both afterbody-on and afterbody-off configurations and for smooth and rough surface conditions. Pitching-moment and normal-force coefficients, within the accuracy of the results, were generally observed to be linear functions of angle of attack over the -6° to $+12^\circ$ angle-of-attack range investigated. The linearity was unaffected by removal of afterbody or change in surface condition. The principal limitation on the accuracy was the stream angularity present at the higher Mach numbers and this was sufficient (about 0.4°) to possibly conceal small nonlinearities.

For both of the shapes tested, the values of pitching-moment slope with angle of attack fell close to unmodified Newtonian values. Normal-force curve slope was predicted within 15 percent by unmodified Newtonian theory.

INTRODUCTION

The tests reported herein were initiated from a free-flight investigation, conducted in the Ames supersonic free flight wind tunnel, of the dynamic stability of two blunt-nosed bodies of revolution of low fineness ratio at Mach number 4. Previous tests in the Ames Unitary Plan wind tunnel reported in reference 1 showed the existence of unstable damping in pitch for these bodies at moderate supersonic speeds. In order to

*Title, Unclassified

analyze the motions of the models in flight it is necessary to determine whether there are significant nonlinearities in the static pitching-moment characteristics. Reference 2 illustrates by means of a simple mechanical analog the effect of nonlinearity of pitching moment on the motion of a free-flight model. This effect on the motion is important both in reducing free-flight data and in predicting the trajectory of a full-sized body. Therefore, it was deemed necessary to determine the variation of pitching moment with angle of attack. For this investigation, the Ames 1- by 3-foot supersonic wind tunnel No. 1 was used.

SYMBOLS

C_m pitching-moment coefficient about model center of gravity, $\frac{\text{pitching moment}}{qSd}$

C_{m_α} $\frac{dC_m}{d\alpha}$, per radian

C_N normal-force coefficient, $\frac{\text{normal force}}{qS}$

C_{N_α} $\frac{dC_N}{d\alpha}$, per radian

d maximum diameter of model

M free-stream Mach number

q free-stream dynamic pressure

R Reynolds number, based on free-stream properties and base diameter

S reference area, $\frac{\pi d^2}{4}$

x,y body coordinates (see fig. 1)

α angle of attack

APPARATUS AND TESTS

The two blunt-nosed bodies tested in this investigation are illustrated in figures 1 and 2. The models are similar in that each has a blunt nose followed by a conical afterbody (the significant difference being in the shape of the nose). The nose of the first model is a paraboloid of revolution and was intended to represent the round-nosed cone approach to the design of high drag shapes. This model will be referred to as the round-nosed model in the report. The nose of the second model is a section of a sphere of large radius followed by a short conical flare. Since the face of this model is nearly flat, it will be referred to as the flat-nosed model. About 80 percent of the tests reported herein were made with this latter model.

To allow separation of the effects of nose shape from the effects of afterbody, the models were constructed in two parts - nose and afterbody. All parts were machined from 2024 aluminum and were given a smooth machined surface. For tests with a rough surface, the entire nose was covered with salt, bonded to the nose with a thin layer of lacquer.

The models were tested in the Ames 1- by 3-foot supersonic wind tunnel No. 1. This tunnel is a closed-circuit continuous-operation type and is equipped with a flexible-plate nozzle that provides a variation of Mach numbers from 1.4 to 4.0. Mach numbers and Reynolds numbers for the present tests were as follows:

Mach number	Reynolds number, million
2.4	0.7 to 1.3
3.3	0.7 to 1.8
4.0	0.7 to 2.0

The models were sting mounted and were tested through an angle-of-attack range of -6° to $+12^\circ$. The angle-of-attack range was increased from 6° to 12° by means of a 6° bent sting. Unfortunately, the center of rotation of the angle-of-attack mechanism was located considerably behind the base of the model and, as a result, the model was translated about 10 inches as the angle of attack was varied (see photographs in fig. 3). This translation subjected the model to air flow in different areas of the test section as the angle of attack was varied.

The forces and moments of these models were measured with an internal, three-component strain-gage balance. For presentation, all forces and moments were transferred to the selected center-of-gravity position of the model indicated in figure 1.

[redacted]

ACCURACY

The major source of error in the results is believed to be caused by unknown stream angularity; there was no stream-angle survey available for the vertical plane of the test section through which the model was translated. A stream-angle survey was available for the horizontal plane which gave a maximum angular deviation of the flow of 0.4° at $M = 4.0$. If it is assumed that this degree of stream angularity is present in the vertical plane also, and if the effect of the stream angle is simply viewed as causing an error in angle of attack, then errors in α of up to 0.4° due to this cause might be expected. With this assumption, the accuracy of the experimental coefficients is estimated and shown below.

C_m	± 0.003
C_N	$\pm .005$
C_{m_α}	$\pm .01$
C_{N_α}	$\pm .02$
M	$\pm .03$

RESULTS AND DISCUSSION

The results of this test are plotted in the following figures:

C_m as a function of α, figures 4(a) to (f)
C_N as a function of α, figures 5(a) and (b)
C_{m_α}, C_{N_α} as a function of M, figure 6

As shown in figures 4 and 5 there appear to be nonlinearities in the variations of C_m and C_N, with angle of attack, primarily at $M = 4.0$. To determine whether this results from change in angle of attack or from change in test section position (stream angle effect), data for the flat-nosed model at $M = 4.0$, $R = 2.0 \times 10^6$ are plotted in figure 4(a) for both the -6° to $+6^\circ$ range and the 0° to 12° range. The data for $\alpha = -6^\circ$ to $+6^\circ$ are symmetrical about the origin, and the data for $\alpha = 0^\circ$ to 12° are symmetrical about a point at $\alpha = 6^\circ$. This indicates that the apparent nonlinearity is due principally to stream angularity in the tunnel, since the deviations in the data are a function of model position in the test section and independent of the angle of attack. The maximum effective change in stream angle is apparently about 0.4°, which agrees with the maximum stream angle measured in the horizontal plane of this test section.

At $M = 4.0$, comparisons of pitching-moment results for changes in afterbody configuration and surface condition are given in figures 4(b) and (c) for the flat-nosed model. In figure 4(b), a comparison is made

[redacted]

for afterbody-on and afterbody-off conditions for a model with a roughened surface. As shown, there is little effect on C_m caused by removing the afterbody. In figure 4(c) a comparison is made for afterbody-on and afterbody-off conditions for a model with a smooth surface. Again, there is little effect of the afterbody. In addition, it should be noted that the line drawn through the data in figure 4(c) has the slope determined from figure 4(b). From this it is evident that roughening the surface had negligible effect on the pitching moment.

The effect of Mach number on the variation of C_m with angle of attack for the flat-nosed model is shown in figure 4(d). The slope of C_m with α is seen to increase with a decrease in Mach number. At Mach numbers 2.5 and 3.3, indications from the results are that the air stream is much better than that at $M = 4.0$. The air-stream survey from the horizontal plane indicates that this is true also.

All of the above data are shown to be linear within the test accuracy. There was, however, one instance in which the data did not conform to the usual pattern. These data for the flat-nosed model at $M = 2.36$ are plotted in figure 4(e). Here, the slope of C_m with α is much steeper at $\alpha = 0$ ($C_{m_\alpha} = -0.309$) than the average slope ($C_{m_\alpha} = -0.225$). These results can be compared to the results at $M = 2.5$ of figure 4(d) which show a different curvature about $\alpha = 0$. The difference between these two tests is primarily a change from a smooth to a rough surface, which evidently did have, in this case an effect on C_{m_α} at small angles of attack.

The preceding data were for the flat-nosed model, the shape for which most of the testing time was devoted. An example of data recorded for the round-nosed model is shown in figure 4(f). These data, at $M = 3.3$, $R = 1.8 \times 10^6$, are seen to be linear in nature.

The variation of C_N with α is shown in figure 5(a) for the flat-nosed model and in figure 5(b) for the round-nosed model. These data can be seen to be linear within the accuracy of data from 0° to 12°.

Values of C_{m_α} and C_{N_α} are shown in figure 6 for both shapes and for afterbody-on and afterbody-off conditions with both rough and smooth surfaces. Because of the irregularity in the data, a method of least squares fit was applied to obtain the best straight line fit to the data for the full range of angles of attack. The values of C_{m_α} and C_{N_α} observed from these tests are compared to unmodified Newtonian values as computed from reference 3. The agreement for C_{m_α} for both bodies between unmodified Newtonian values and experimental values is good. For C_{N_α} unmodified Newtonian theory agrees closely with experimental results for the flat-nosed model, but overestimates experimental results by 15 percent for the round-nosed model. The variation of C_m and C_N and C_{m_α}

and C_{N_α} with change in Reynolds number is not shown because there was no discernible effect of a change of Reynolds number over the range investigated.

CONCLUSIONS

Two blunt-nosed shapes were tested through an angle-of-attack range of -6° to $+12^\circ$ for Mach numbers from 2.4 to 4.0 and Reynolds numbers, based on base diameter, from 0.7 to 2.0×10^6. As a result of these tests, these conclusions are reached.

1. Within the accuracy of the data, pitching-moment and normal-force coefficients, C_m and C_N, generally vary linearly with angle of attack from -6° to $+12^\circ$ and their mean slopes, C_{m_α} and C_{N_α}, appear to be unaffected by changes in afterbody configuration, surface condition, or Reynolds number.

2. Values of C_{m_α} for both bodies and C_{N_α} for the flat-nosed body are predicted closely by unmodified Newtonian theory. For the round-nosed body, C_{N_α} computed from Newtonian theory was about 15 percent greater than the measured values.

Ames Research Center
National Aeronautics and Space Administration
Moffett Field, Calif., Nov. 4, 1958

REFERENCES

1. Bird, John D., and Reese, David E.: Stability of Ballistic Reentry Bodies. NACA RM L58E02a, 1958.

2. Canning, Thomas N.: A Simple Mechanical Analogue for Studying the Dynamic Stability of Aircraft Having Nonlinear Moment Characteristics. NACA TN 3125, 1954.

3. Tobak, Murray, and Wehrend, William R.: Stability Derivatives of Cones at Supersonic Speeds. NACA TN 3788, 1956.

All dimensions in inches

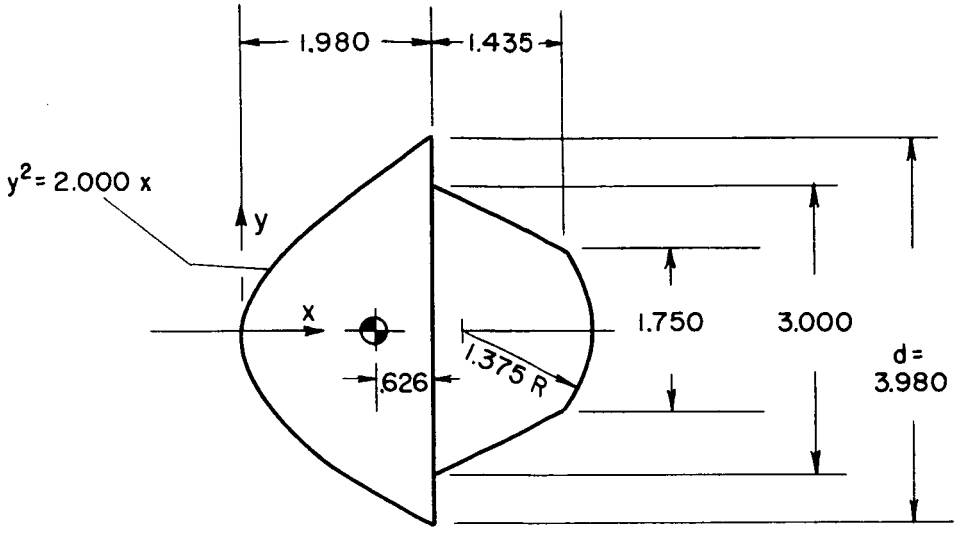

Round-nosed model with afterbody

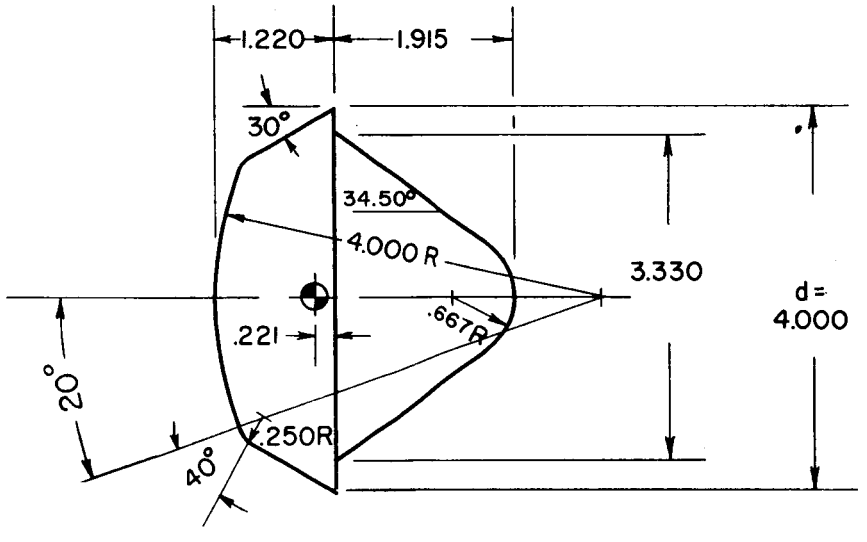

Flat-nosed model with afterbody

Figure 1.- Sketch of models.

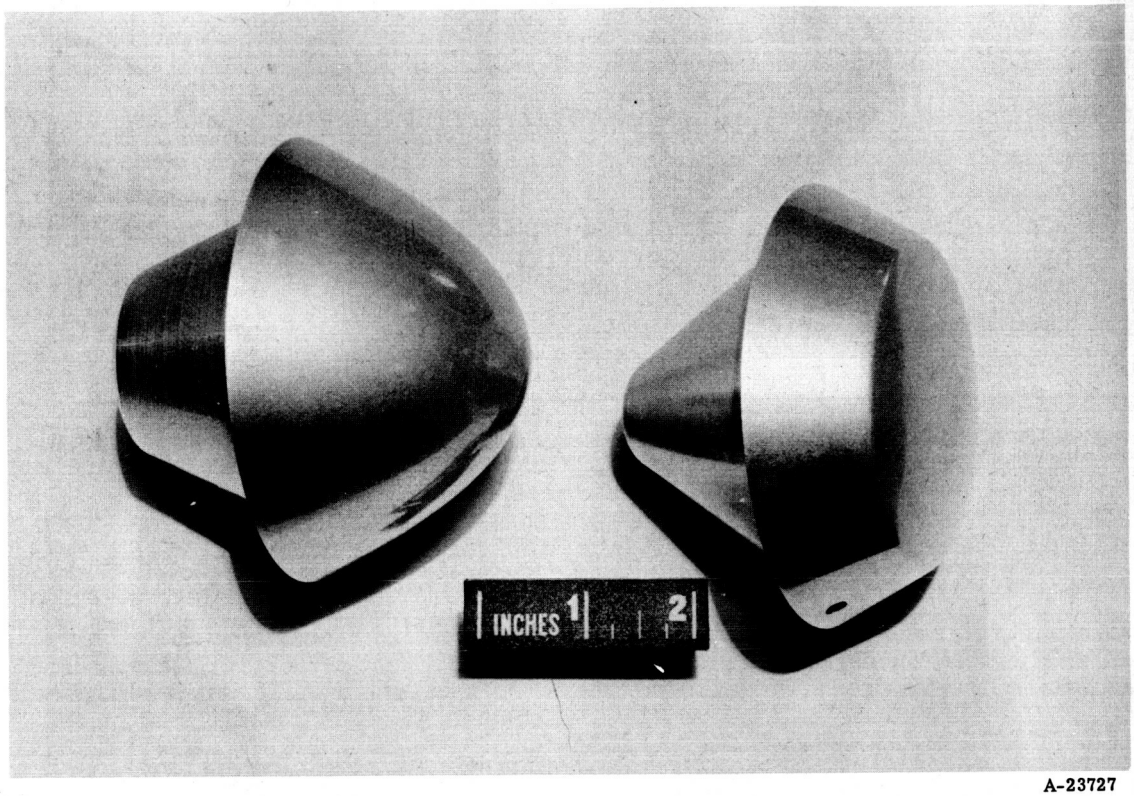

A-23727

Figure 2.- Photograph of models.

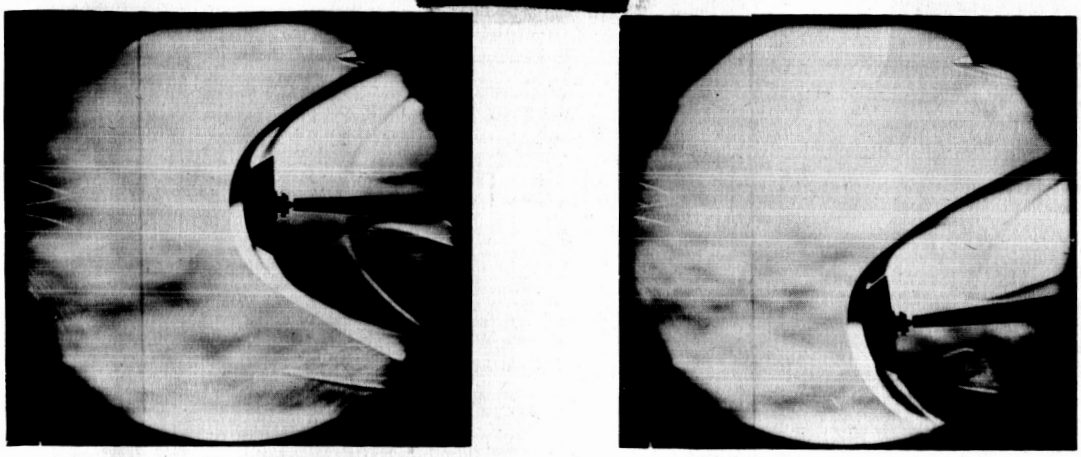

$\alpha = 0^{\circ}$ $\alpha = -6^{\circ}$

(a) Flat-nosed model; afterbody off; smooth surface.

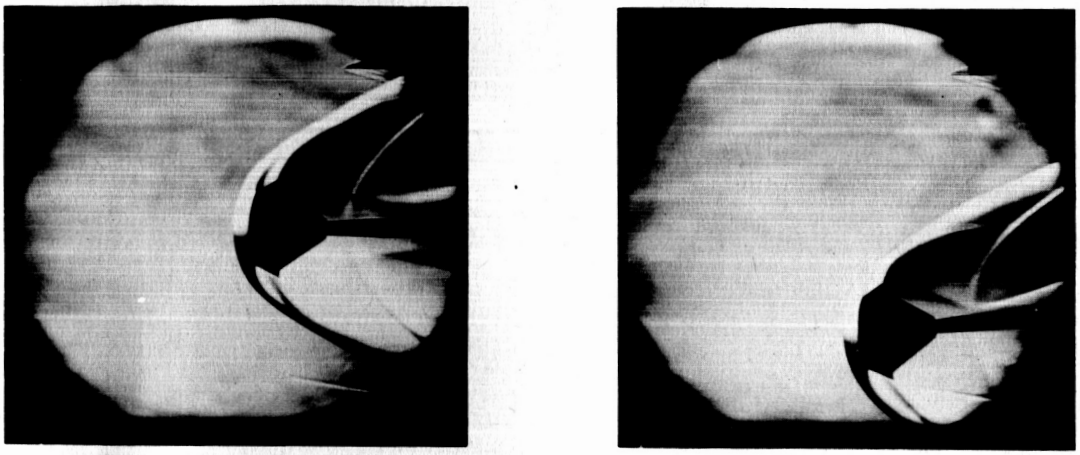

$\alpha = 0^{\circ}$ $\alpha = -6^{\circ}$

(b) Flat-nosed model; afterbody on; rough surface.

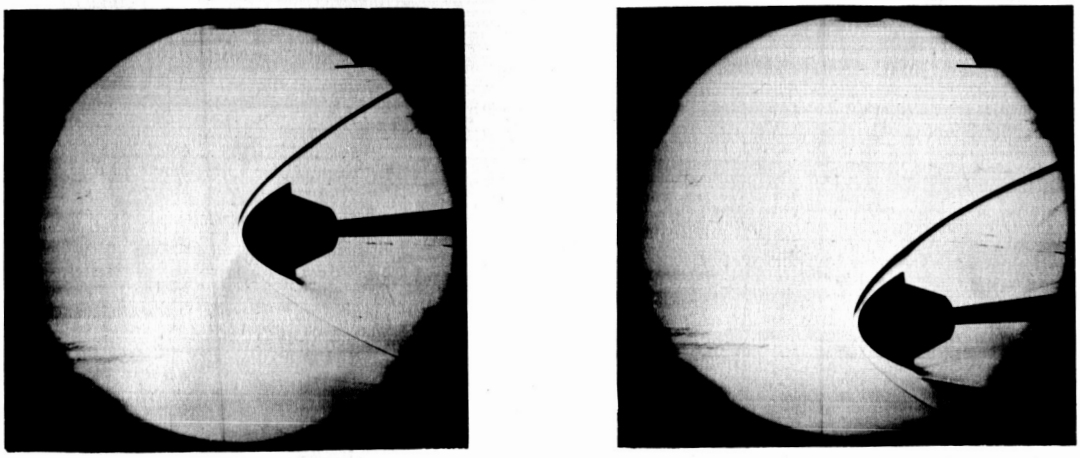

$\alpha = 0^{\circ}$ $\alpha = -6^{\circ}$

(c) Round-nosed model; afterbody on; smooth surface.

Figure 3.- Schlieren and shadowgraph photographs of models in tunnel; $M = 4.0$; $R = 2.0 \times 10^{6}$.

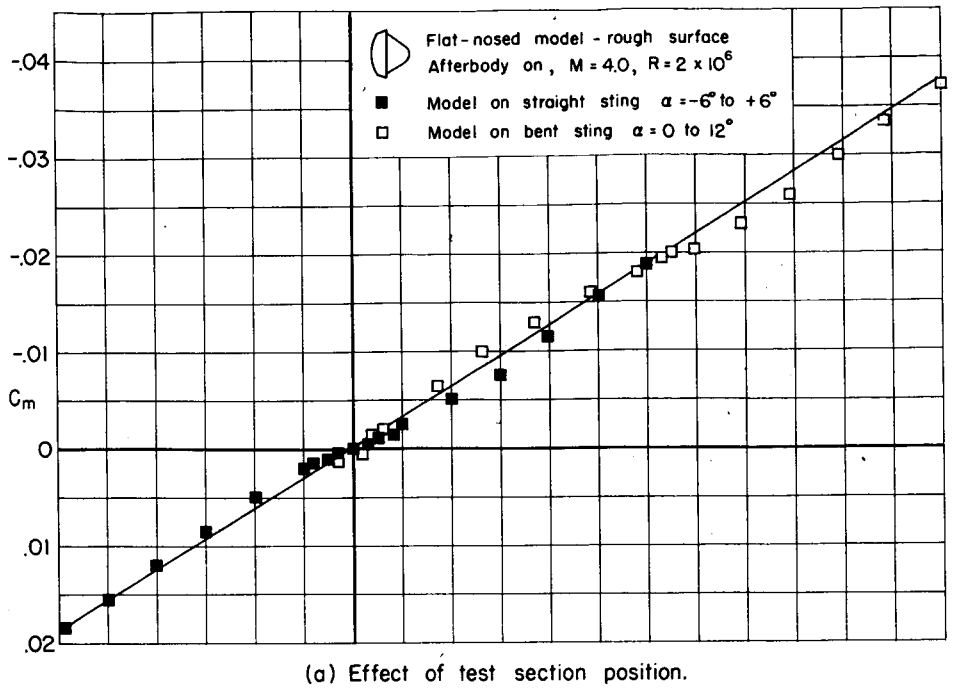

(a) Effect of test section position.

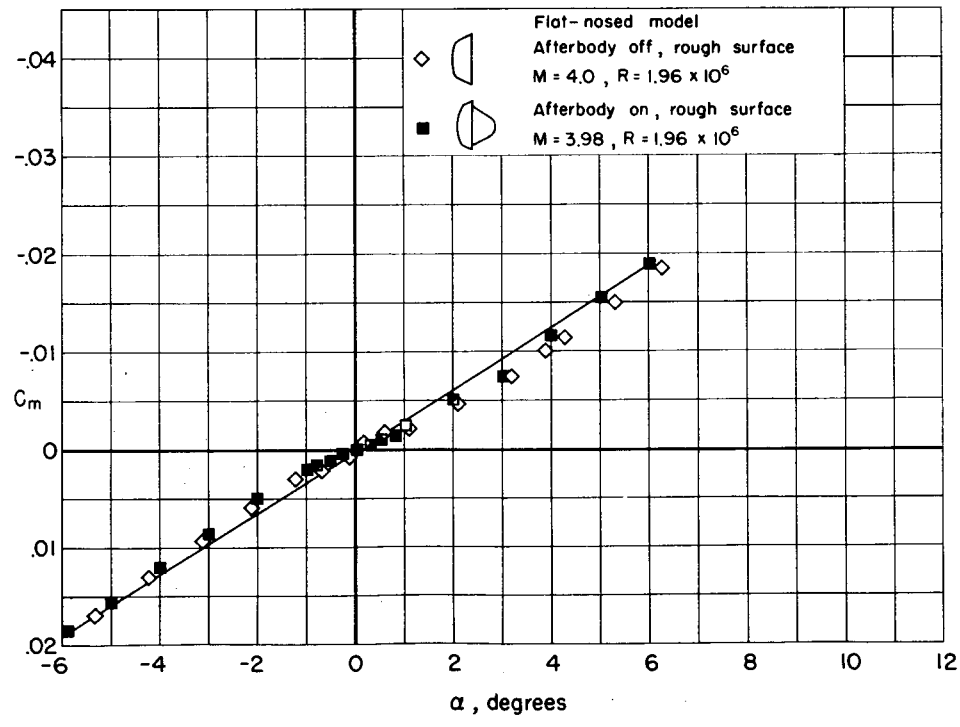

(b) Effect of afterbody with rough surface.

Figure 4.- Variation of pitching moment with angle of attack.

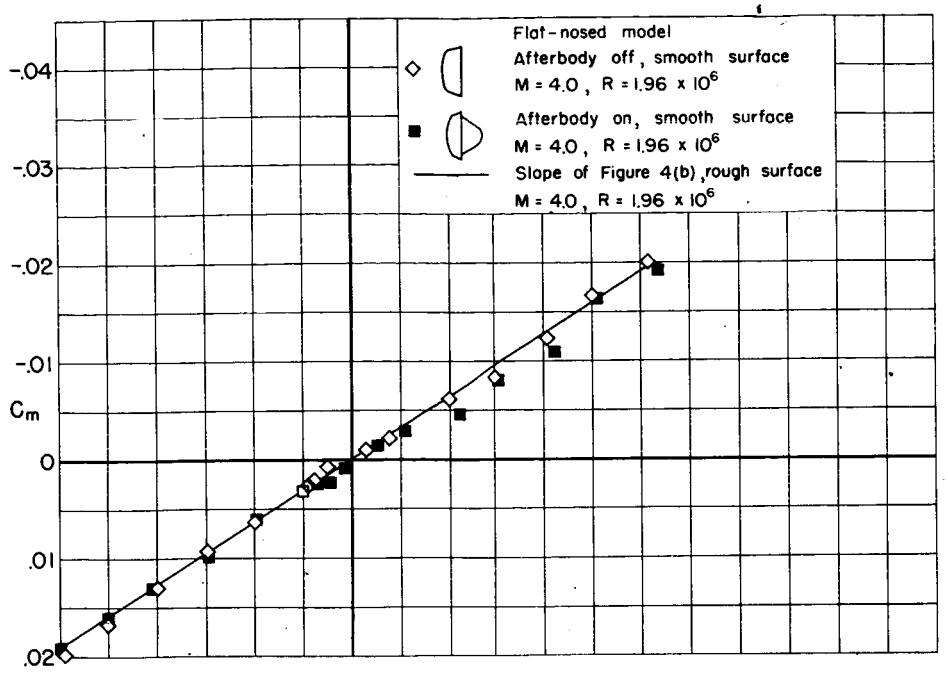

(c) Effect of afterbody with smooth surface.

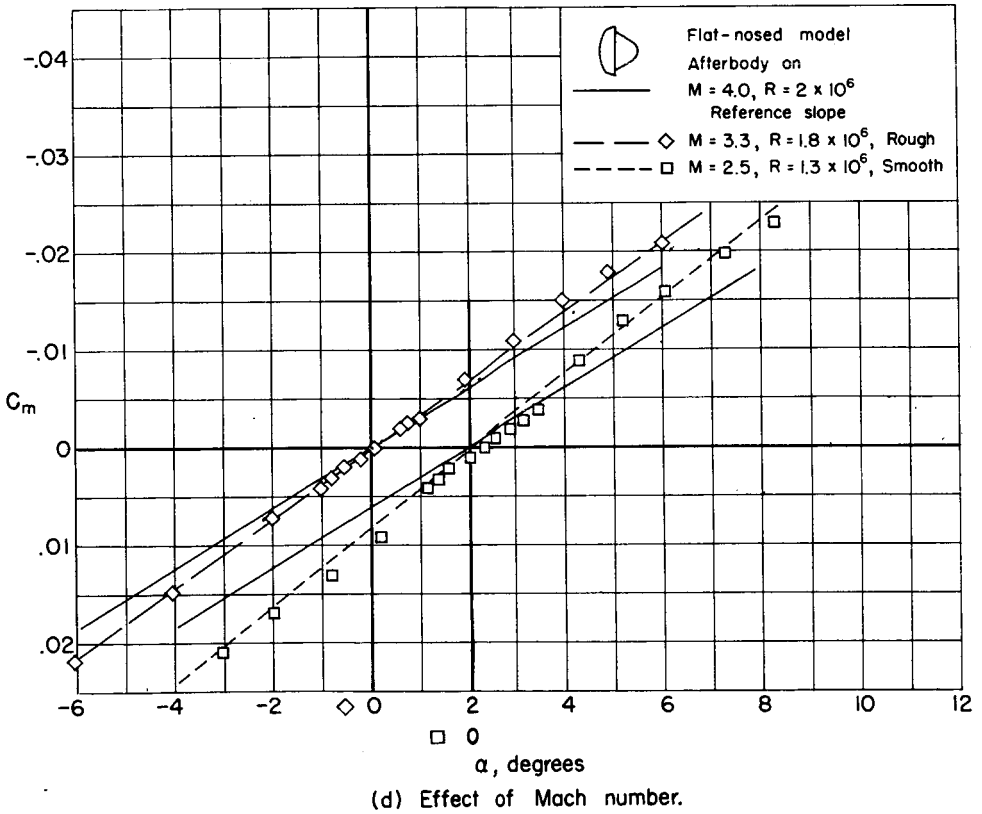

(d) Effect of Mach number.

Figure 4.- Continued.

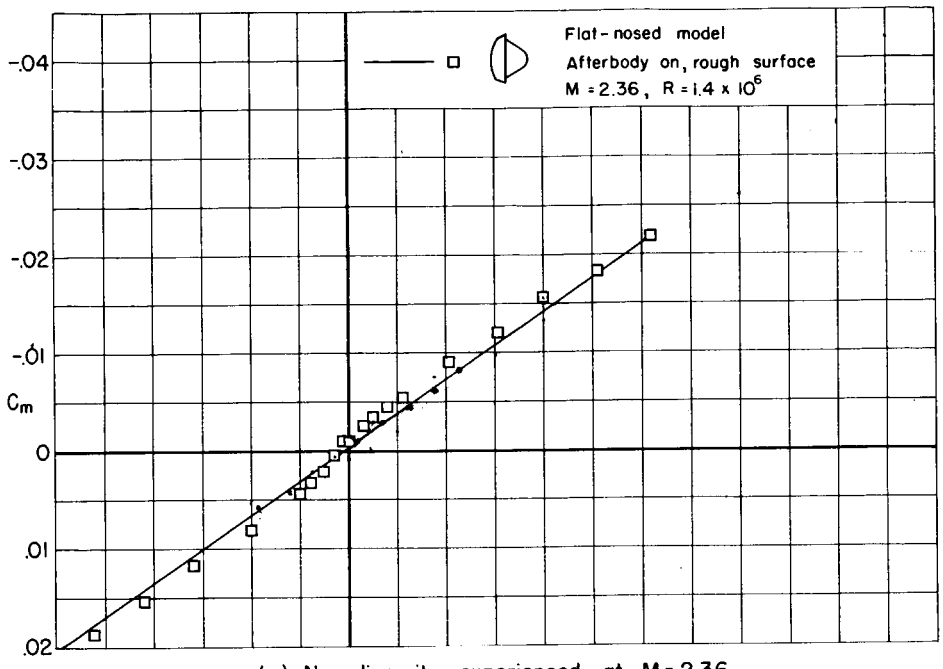

(e) Non linearity experienced at M = 2.36.

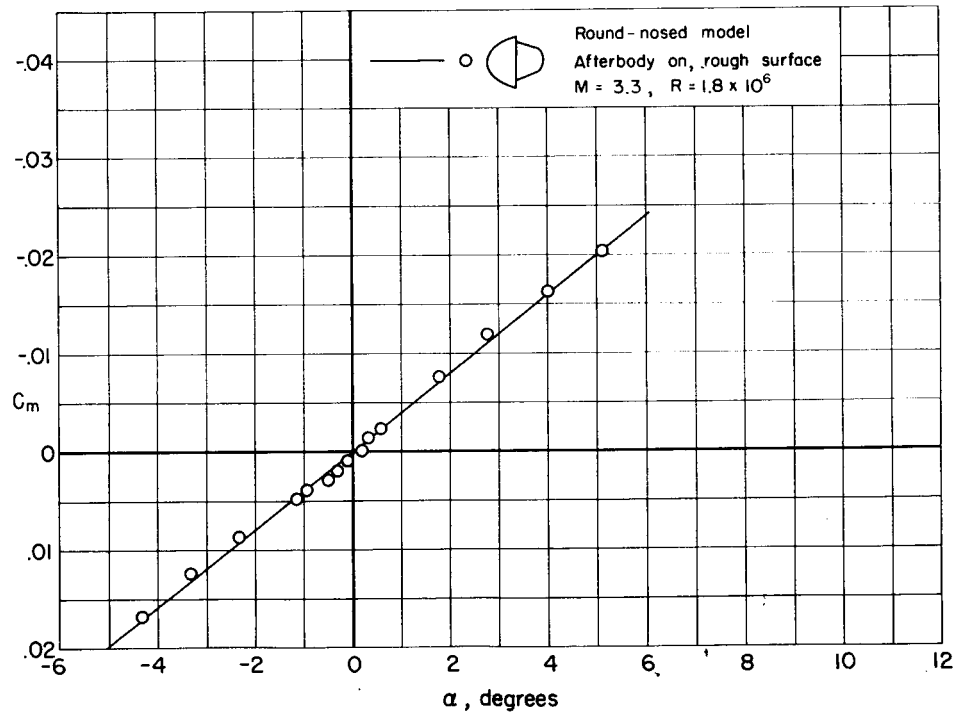

(f) C_{m_α} for round-nosed model.

Figure 4.- Concluded.

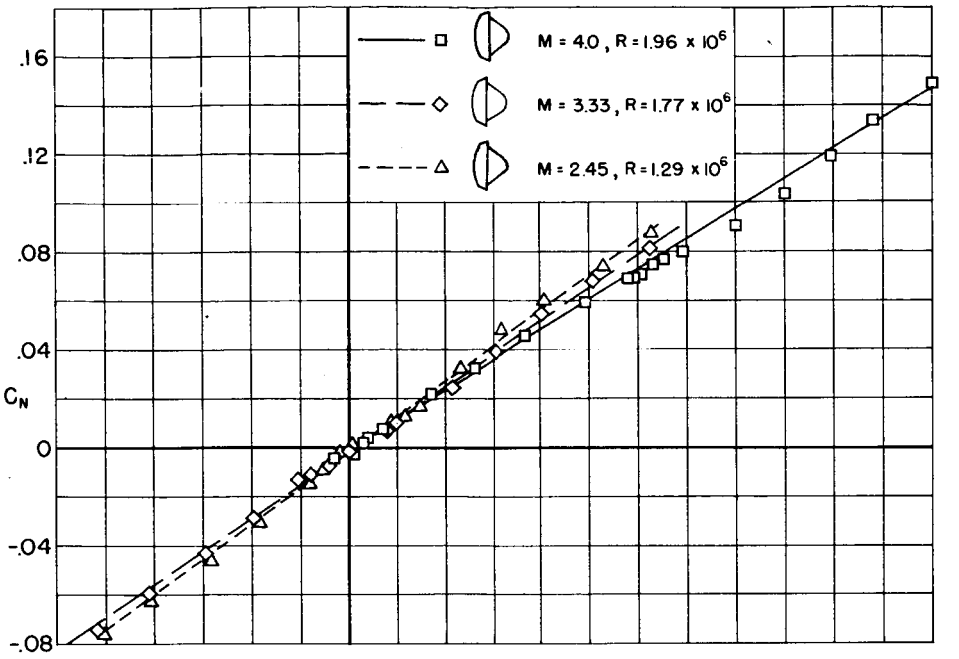

(a) Flat - nosed model.

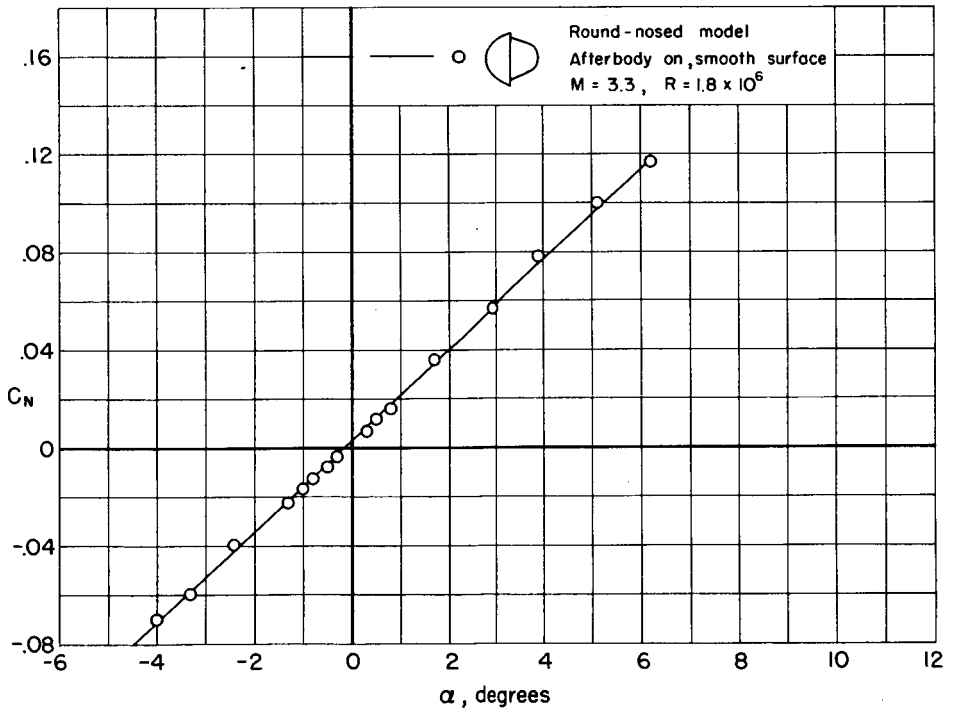

(b) Round - nosed model.

Figure 5.- Variation of normal-force coefficient with angle of attack.

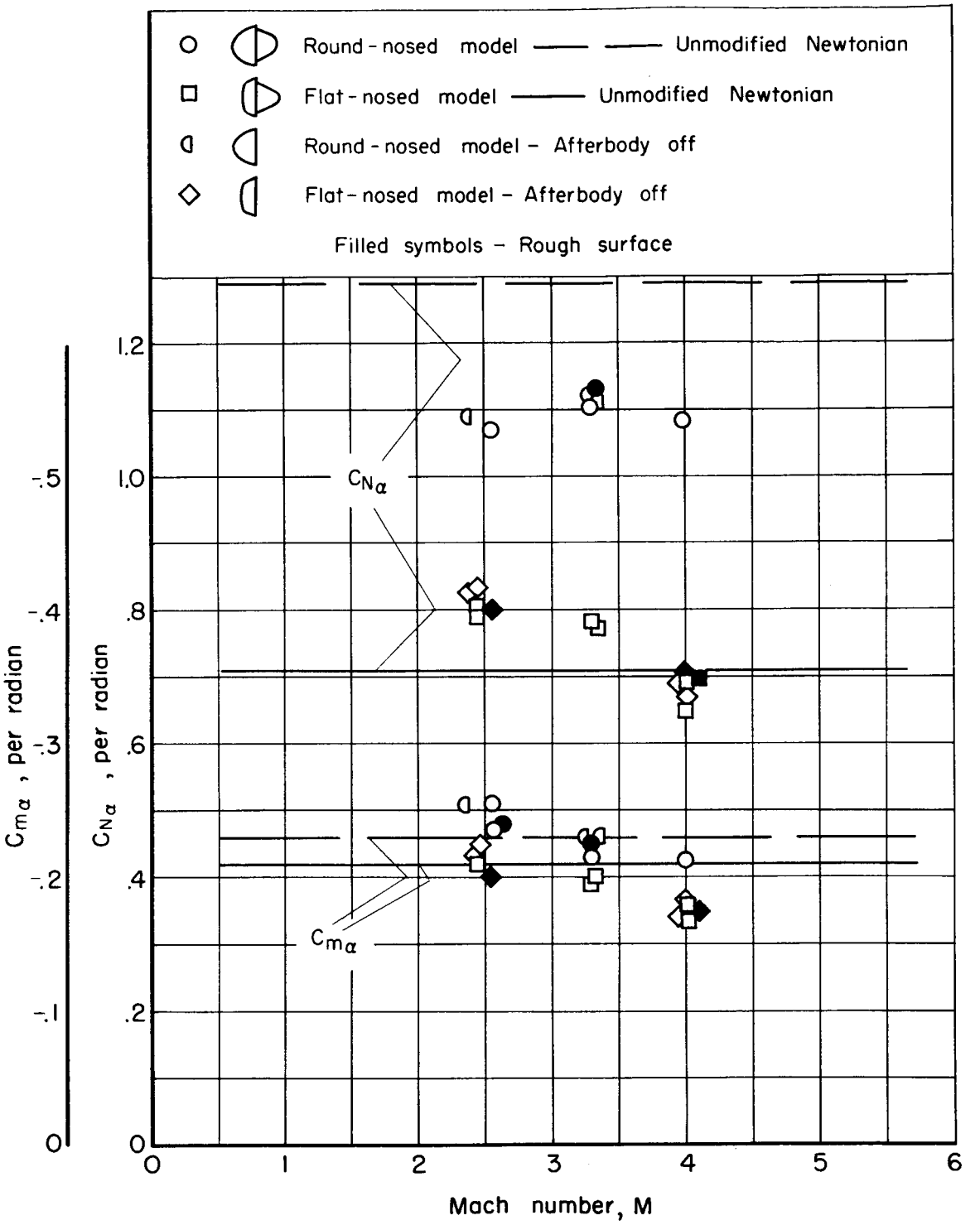

Figure 6.- Variation of C_{m_α} and C_{N_α} with Mach number.